ROYAL SOCIETY
OF CHEMISTRY

www.rsc.org/crystengcomm

Environment friendly template free microwave synthesis of sub-micron sized hierarchical titania nanostructures and their application in photovoltaics

Sofia Javed, Muhammad Aftab Akram, Mohammad Mujahid.

School of Chemical and Materials Engineering, National University of Sciences and Technology, H-12, Islamabad, Pakistan.

Abstract:

A simple low temperature microwave synthesis of hierarchical nanostructures (HNSs) of titania in DI water is reported. A great advantage of the reported method is the production of sub-micron sized HNSs without any surfactant or hydrofluoric acid. The hierarchical morphology provides huge surface area for maximum exposure for light driven reactions and 3 D folding morphology allows further scattering of light to get its maximum utilization. FESEM, TEM, XRD, BET surface area measurement, UV/VIS and raman spectroscopy were utilized to understand the structures. Mechanism of formation of nanostructures is also discussed. The nanostructures were employed in Dye Sensitized Solar Cells for performance comparison.

Keywords: Titania nanoflowers, microwave synthesis, hierarchical nanostructures.

Titania nanostructures being thermally and chemically stable, cheap and nontoxic[1, 2] offer their potential for use in various applications including photocatalysis[3-5], photovoltaics[6, 7], gas sensors[8, 9], adsorbents, supports and many others[10]. Among various nanostructures of titania, the synthesis of nanoparticles/spheres[6, 11], nanobelts[12], nanorods[7, 13], nanowires[14] and nanotubes[15] can be found in a number of reports in the literature but relatively few reports can be found on the synthesis of hierarchical nanostructures(or nanoflowers) of titania[9, 14, 16-19]. The hierarchical morphology offers large specific surface area (enabling greater generation and migration of photocarriers from adsorbed species on the surface), light absorption improvement and high refractive index (enabling higher light absorption and refraction), hence they offer high photocatalytic efficiency [2]. The reports on the synthesis of HNSs of titania include hydro/solvothermal, microemulsion synthesis, sol gel method, hydrolysis/alkolysis and electrodeposition oxidation methods[2, 9, 14, 16-19]. Generally, the synthesis of titania HNSs makes use of organic/inorganic salts of Ti, surfactants, highly toxic hydrofluoric acid, high temperature and pressures. Most of the reported HNSs produced by the said methods have diameters in the micron ranges, except the microemulsion (using surfactants) and hydrolysis/alkolysis methods (produce smaller nanoflowers) but these methods have issues of difficult control due to many parameters governing the process[2]. Microwave synthesized nanostructures possess high specific surface area, good photo catalytic and redox properties[20]. The microwave synthesis of nano titania with different architectures including nanoparticles[4, 21], nanotubes[5, 12, 20], nanorods[22, 23], nanospheres[23, 24]; has evolved as an instant, efficient and cheap fabrication route. There are a few reports on microwave synthesis of titania HNSs[14, 17]. R. Rahal et al. have reported the microwave synthesis of titania nanoflowers using TiF_4, template CTAB and urea at a temperature of 120^oC in water, although they have not used the hydrofluoric acid but the surface directing agent plays the main role in the formation of nanoflowers[17]. J. Huang et al. report the formation of titanate nanoflowers on microwave treatment of titania nanopowder under 8M aqueous NaOH at 240^oC for 45 minutes[14].

This report presents an instant economical method to produce HNSs at 1 atm and 100°C in 5 minutes in 10M NaOH aqueous solution. Sub-micron sized HNSs of titania are prepared under environment friendly conditions with no hydrofluoric acid, organic additives and surfactants. Microwave treatment was applied to anatase powder dispersed in aqueous 10M sodium hydroxide solution for different durations (5 minutes to 20 minutes) at a power of 250W.

Table 1 depicts the sample designation with different treatment times along with crystallite sizes calculated from XRD plots using Scherrer equation, degree of crystallinity calculated using XRD peak areas, band gap values measured using UV/VIS spectroscopy[25] (Supporting Information) and BET surface area values for different samples. Figure 1 shows a plot for crustallite size, band gap and surface area with the increasing microwave exposure. Although anatase phase of titania has a band gap of 3.2eV, the high band gap values obtained here for all the samples can be attributed to the small crystallite size of the starting material[26]. The band gap and the surface area are decreasing as the microwave treatment time increases and the crystallite size is increased with increase in microwaves exposure time.

Sr. No.	Sample ID	Treatment duration (minutes)	Crystallite size(nm) (XRD)	Degree of crystallinity	Band Gap (eV)	BET surface area (m^2/g)
1.	T1	0	5.6	0.85	3.83	191
2.	MT2	5	7.2	0.62	3.75	82
3.	MT3	10	10.1	0.79	3.7	68
4.	MT4	15	13.0	0.79	3.67	25
5.	MT5	20	13.8	0.66		18

Table 1: Crystallite size, degree of crystallinity, band gap and BET surface area values for different samples treated with microwave radiation for different durations.
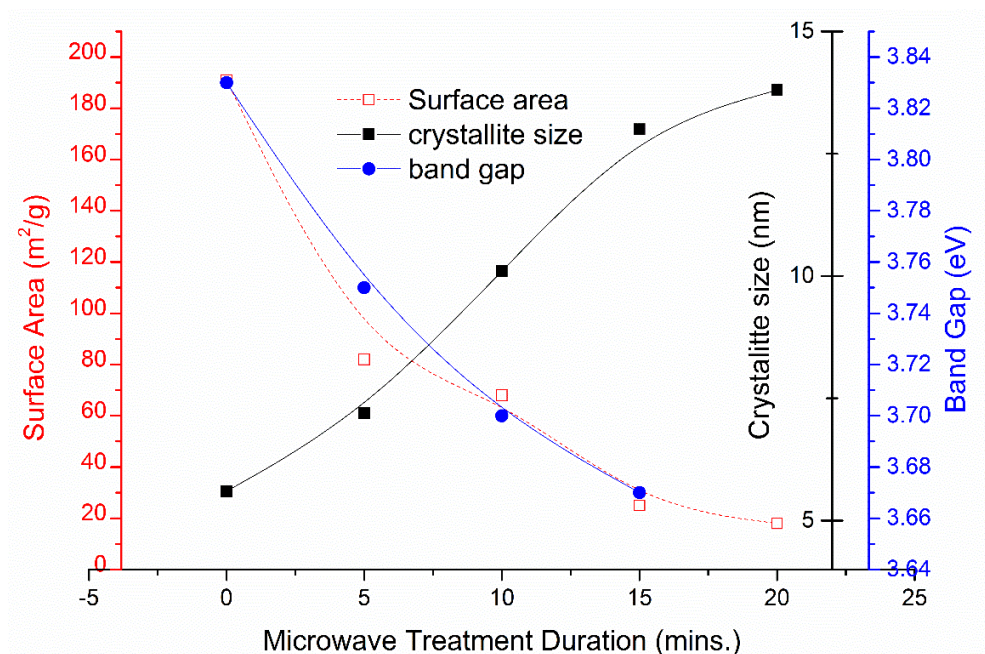
Figure 1: Variation of band gap, crystallite size and surface area with microwave treatment duration of 0, 5, 10, 15 and 20 minutes.

As stated earlier, the starting material is anatase phase of titania. The titania quantum dots with crystallite size around 5nm was prepared by sol gel reflux synthesis described in our previous report[11]. The small crystallite size has resulted in the formation of small HNSs (nanoflowers) in all the samples after microwave treatment without use of any surfactant. The small sized HNSs are advantageous for offering huge surface area and retaining the light trapping effects for better efficiencies in photocatalytic devices.
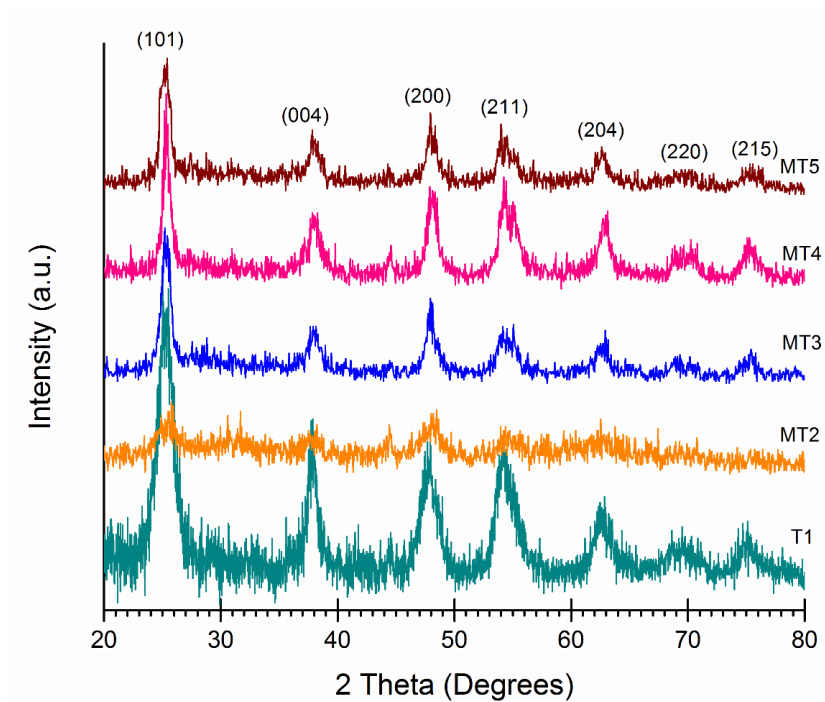

Figure 2: XRD plots of starting material T1 and microwave treated samples MT2 (5 min), MT3 (10 min), MT4 (15 min) and MT5 (20 min) after annealing at $450^{o}C$ for 1 hour.

The XRD plots as shown in figure 2 reveal that the anatase phase is the major crystalline phase in all the samples with different microwave treatment durations. All peaks match with those of tetragonal anatase phase with space group I41/amd and are indexed (reference code: 01-071-1168).

FESEM images for the starting material and the treated samples are shown in figure 3. Titania HNSs of sizes around 500nm can be observed. With increase in the microwave treatment from 5 minutes
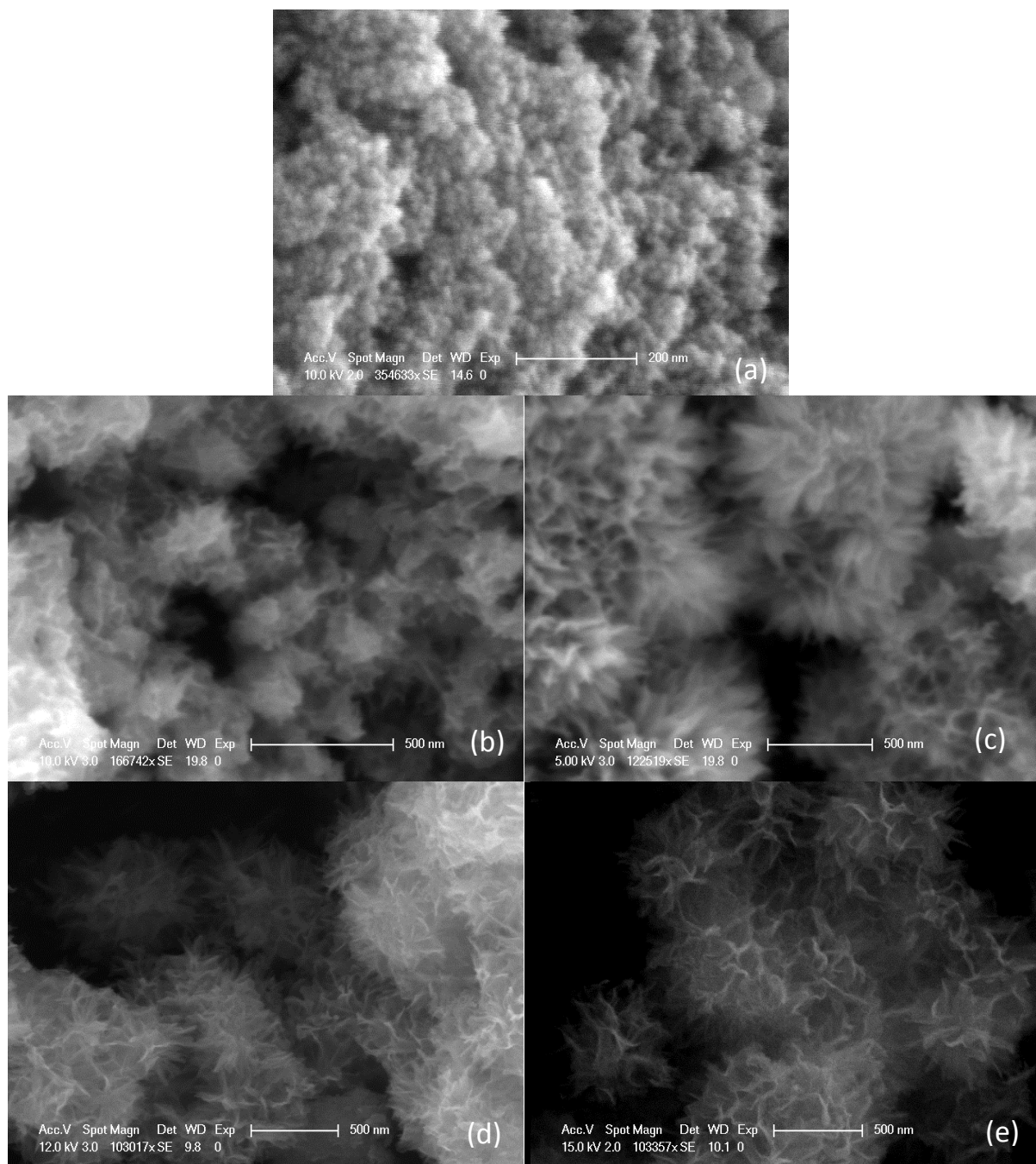
Figure 3: FESEM images of titania nanostructures T1 (a) MT2 (b), MT3 (c), MT4 (d), MT5 (e)

to 20 minutes the morphology is gradually becoming sharper with little or no effect on the sizes of the HNSs.

Figure 4 shows the TEM images of MT2 and MT4. Here we can observe that the HNSs are made up of somewhat radially arranged nanosheets. With the increase in the treatment time the nanosheets have twisted and rolled along their sides. This can be related to the formation mechanism of nanotubes

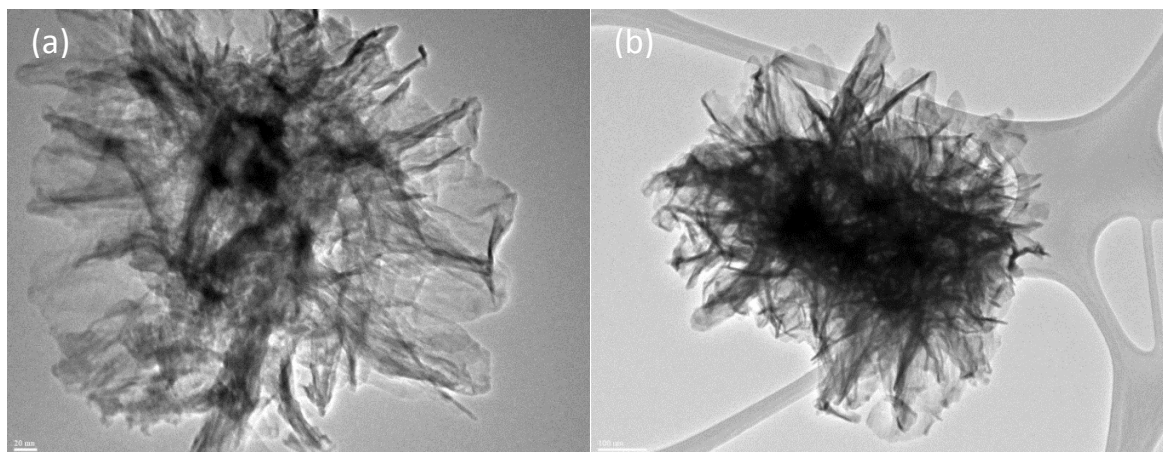*Figure 4: TEM images of Hierarchical nanostructures of Titania MT2 (a) and MT5 (b)*

with same contents under hydrothermal conditions[27]. It should be mentioned here that although the synthesis conditions are similar to the formation of nanotubes under hydrothermal treatment but the HNSs are stable as the results shown in this report are all obtained after annealing of the treated samples at $450^{o}C$ for 1 hour. The formation mechanism of these HNSs will be discussed later. From TEM the crystallite size is not quantifiable. The crystallite size calculated from XRD plots using the Scherrer equation maybe called the effective crystallite size of the corresponding samples.
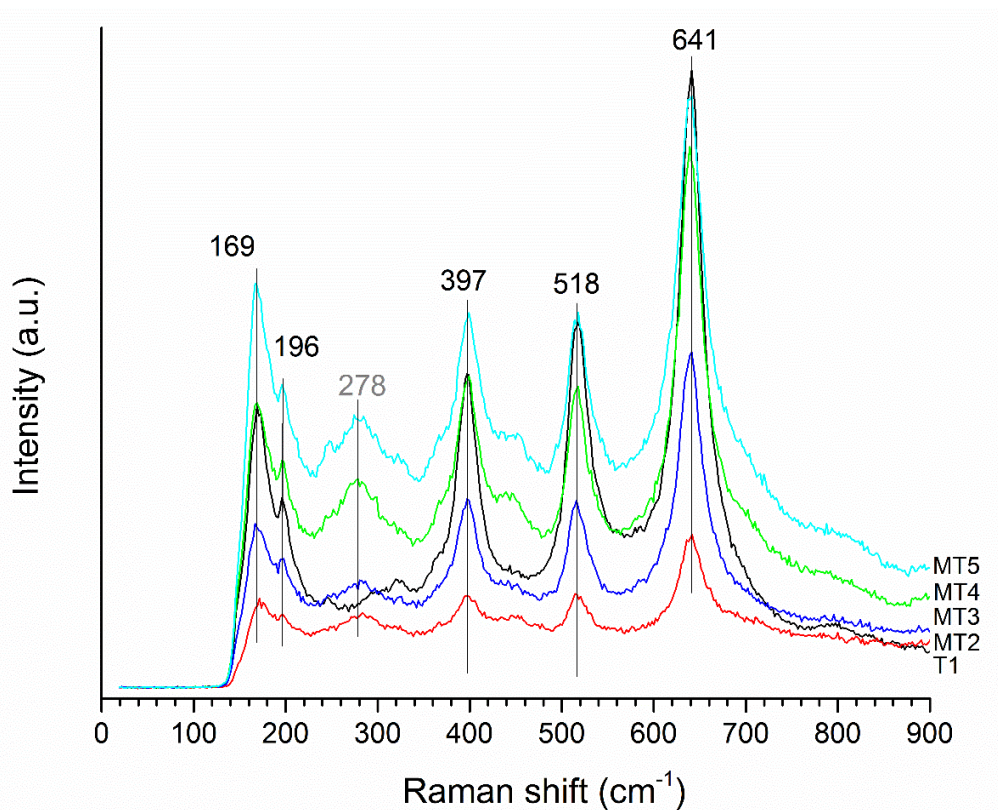

Figure 5: Raman spectra of titania HNSs MT2, MT3, MT4, MT5 and the starting nanopowder T1.

Figure 5 shows the raman spectra for the samples. These have peaks corresponding to the anatase phase of titania. The anatase phase of titania is found with following raman modes: three Eg modes at 169 (Eg (1)), 196 and 641 cm^{-1}, two B1g modes at 397 and 518 cm^{-1}. A1g mode at 513 cm^{-1} seems to be embedded in peak at 518 cm^{-1} [28]. The variations in the raman intensity can be related to the variation in the surface roughness of the starting material and those after microwave treatment. The starting sample has ~5nm sized crystallites with ~20 nm particles and shows maximum intensity among the raman spectra as small crystallite size give large shift and broadening of the Raman band[29]. After microwave treatment the surface roughness gradually increases from 5 min to 20 minutes treatment duration and the raman intensity also increases with the increase in treatment duration due to formation of distinct few nanometer thick sheets of the HNSs.

The growth mechanism maybe related to the reported mechanism for the formation of titania nanotubes under hydrothermal conditions using titania nanoparticles in 10 M NaOH solution, i.e. on dissolution of the starting titania nanoparticles under highly alkaline medium and under hydrothermal atmosphere, nanosheets are formed which afterwards roll over to make titania nanotubes [27]. In the present case, the situation is somewhat different in that a small duration exposure to microwaves is provided for the same contents at atmospheric pressure. In this situation, it is speculated that the surface of the starting titania nanoparticles begins to dissolve. Subsequently, regrowth occurs on the particles in the form of sheets giving rise to hierarchical morphology.

The increase in crystallite size and consequent decrease in surface area and band gap values upon evolution of the HNSs with increasing microwave exposure is justified. The crystallinity[25] values are calculated using XRD peak areas and are given in the table 1. It is indicated that the crystallinity decreases after 5 minutes microwave exposure owing to more dissolution than regrowth. Then increases till 15 minutes treatment due to increased regrowth of the sheets in the HNSs. On 20 minutes exposure, although the crystallite size has increased, the decrease in crystallinity can be explained by considering random orientation of the planes in the rolling sheets of HNSs, with respect to the incident X-rays. We can see from SEM that the morphology of the HNSs seems to be going to the depth on increasing the microwave treatment duration from 5 minutes to 20 minutes. Also the TEM images can reveal that the MT2 sample seems to have some unchanged central zone while for the sample MT5 the conversion seems to be nearly completed. A schematic illustrating the speculated growth mechanism is given in figure 6.
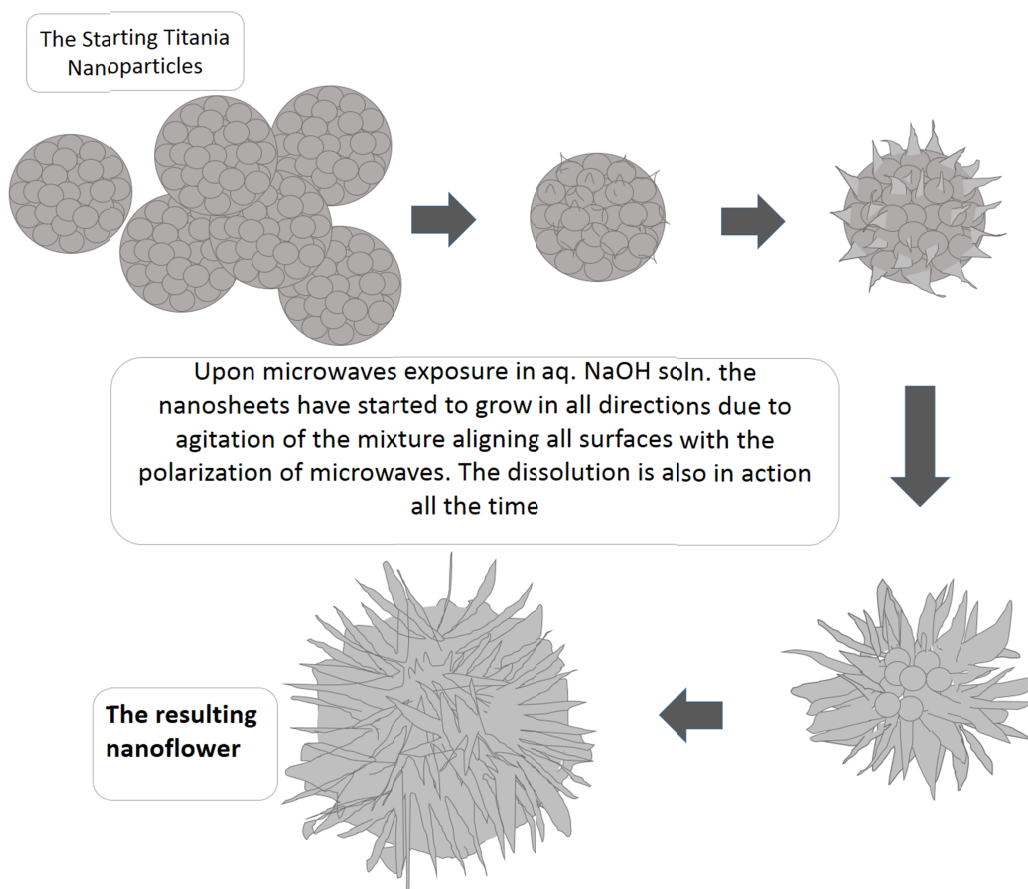
Figure 6: Schematic for the growth mechanism of titania HNSs

It should be mentioned that under the microwave treatment of titania nanoparticles, the 3D morphology is thought to be the result of a role played by microwaves specifically. Titania particles start to dissolve and due to polarization effects of the radiation they regrow three dimensionally in the form of sheets giving nanoflowers like structures. With increase in the treatment duration the depth of the twisted nanosheets seem to be increased due to more and more dissolution of starting material and growth of the sheets as evident from the TEM images (fig. 4).

In order to check the role of microwaves; an experiment, in which reflux condensation at 100°C, was carried out for the same contents but outside the microwave oven for a duration of 20 minutes. In another experiment titania powder in 10M NaOH was heated in a sealed vessel at 100°C for 20 minutes i.e. under hydrothermal conditions. The treated powders were washed several times with DI water and annealed at 450°C for one hour. HNSs were not formed in both these experiments (supporting information). This reveals that microwave treatment under atmospheric pressure is playing main role in producing HNSs without using any template and hazardous chemicals like HF or H_2O_2.

All the microwave reactions were carried out in a domestic oven under refluxing using the assembly shown in the schematic (fig. 7). The commercial microwave reactor cannot be used for highly alkaline media due to exploding hazard of the sealed pressurized reactor vessel.
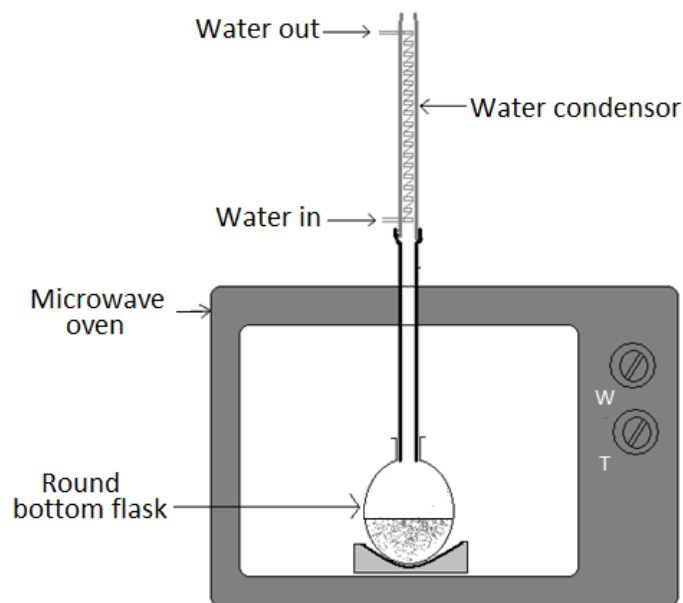
Figure 7: Schematic illustrating the experimental setup for microwave treatment of different samples.

The HNS were employed in DSSCs in comparison with the starting material T1. FTO coated glass slides were cleaned and a blocking layer of titania was fabricated by spin coating a 2% solution of titanium tetraisopropoxide in isopropanol. Pastes of the synthesized titania powders and T1 were made and films were fabricated by doctor blade method. A monolayer of N719 dye was infused on titania films by overnight soaking of the titania coated FTO glass slides in the dye solution. Pt counter electrodes were used. Liquid iodide/triiodide electrode was filled in between the two electrodes. JV measurement was obtained under 1 sun illumination. Figure 8 shows the JV curves for the DSSCs having T1, MT2, MT3 and MT4 as the semiconductor layer. Table 2 gives the fill factor, open circuit voltage, short circuit current density and efficiency values for the devices. Maximum efficiency of 0.1% is achieved with the sample MT2 i.e. HNSs produced after 5 minutes microwave exposure.

The open circuit voltage is maximum for device with T1 and is decreasing for MT2, MT3 and being minimum for MT4. This decrease can be explained considering the decrease in band gap of the samples with increasing microwave exposure. V_{oc} for DSSCs is dependent on the difference between the redox potential of the electrolyte and the conduction band of titania[30]. With decrease in band gap of titania powders the conduction band seems to be lowered resulting in the decrease in V_{oc} in DSSCs. The current density is exhibiting an increase with evolution of hierarchical morphology upon microwave treatment. But as the surface area is also decreasing with increased microwave exposure the net current density is decreased after 5 minutes. The sample MT2 has reasonably high surface area i.e. 82 m^2/g (table 1) with a morphology that is a mix of nanoparticles contributing in surface area and radially arranged nanosheets for greater light absorption giving maximum current density among all. Samples MT3 and MT4 have low surface areas of 24 m^2/g and 18 m^2/g (table 1) so these are showing low current densities in DSSCs. These samples may perform better when used in combination with nanoparticles to combine the light scattering effects of hierarchical morphology and huge surface area of the nanoparticles.
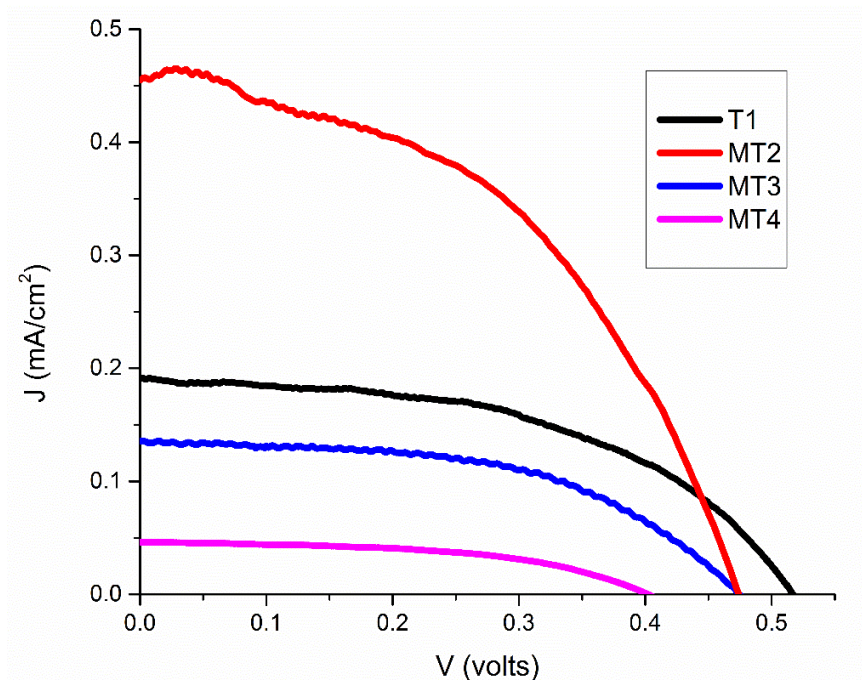
Figure 8: JV curves for DSSCs employing T1, MT2, MT3 and MT4 as semiconductor layer.

Sr. No.	Sample	ff	V_{oc} (Volts)	J_{sc} (mA/cm^2)	η (%)
1.	T1	0.49	0.5174	0.1915	0.0489
2.	MT2	0.48	0.4739	0.4647	0.1055
3.	MT3	0.53	0.4748	0.1356	0.03395
4.	MT4	0.51	0.4036	0.0461	0.00955

Table 2: Photovolatic parameters determined from JV curves of DSSCs employing synthesized hierarchical nanostructures and starting titania.

Conclusion:

We have presented an environment friendly instant microwave method of making hierarchical nanostructures of titania with sizes less than 1 micron. HNSs are produced on the microwave treatment of titania (anatase) powder in 10 M NaOH aqueous solution at 1 atm and 100°C for small durations ranging from 5 minutes to 20 minutes. The specialty of this report is to present a method of making titania HNSs without using hazardous chemicals and high temperatures and pressures. XRD, FESEM, TEM and raman spectroscopy are utilized for understanding the structures. These sub-micron titania hierarchical nanoflowers are then employed in DSSCs for performance comparison with the starting material. The sample after 5 minutes microwave treatment having a surface area of 82 m^2/g, a mixture of nanoparticles and hierarchical morphology show maximum efficiency of 0.1 %. The samples with longer microwave treatment have relatively low surface areas due to conversion to hierarchical morphology and hence are unable to give better performance when used alone. A mix nanoparticle and hierarchical morphology is beneficial for scattering and thus greater absorption of light with large surface area for better performance of the DSSCs.

Acknowledgement:

References:

1. V. Gomez, A. M. Balu, J. C. Serrano-Ruiz, S. Irusta, D. D. Dionysiou, R. Luque and J. Santamaria, *Appl Catal a-Gen*, 2012, **441**, 47-53.
2. Z. Wu, Q. Wu, L. Du, C. Jiang and L. Piao, *Particuology*, 2013.
3. D. Kong, J. Z. Y. Tan, F. Yang, J. Zeng and X. Zhang, *Applied Surface Science*, 2013, **277**, 105-110.
4. S. Sitthisang, S. Komarneni, J. Tantirungrotechai, Y. Dong Noh, H. Li, S. Yin, T. Sato and H. Katsuki, *Ceramics International*, 2012, **38**, 6099-6105.
5. Y. P. Peng, S. L. Lo, H. H. Ou and S. W. Lai, *Journal of hazardous materials*, 2010, **183**, 754-758.
6. C.-Y. Liao, S.-T. Wang, F.-C. Chang, H. P. Wang and H.-P. Lin, *Journal of Physics and Chemistry of Solids*, 2014, **75**, 38-41.
7. M. Zhu, L. Chen, H. Gong, M. Zi and B. Cao, *Ceramics International*, 2014, **40**, 2337-2342.
8. S. Park, S. An, H. Ko, S. Lee, H. W. Kim and C. Lee, *Applied Physics A*, 2013.
9. C. Wang, L. Yin, L. Zhang, Y. Qi, N. Lun and N. Liu, *Langmuir*, 2010, **26**, 12841-12848.
10. B. Choudhury and A. Choudhury, *Materials Science and Engineering: B*, 2013, **178**, 794-800.
11. S. Javed, M. Mujahid, M. Islam and U. Manzoor, *Materials Chemistry and Physics*, 2012, **132**, 509-514.
12. S. Ribbens, V. Meynen, G. V. Tendeloo, X. Ke, M. Mertens, B. U. W. Maes, P. Cool and E. F. Vansant, *Microporous and Mesoporous Materials*, 2008, **114**, 401-409.
13. L. Meng, C. Li and M. P. Santos, *Journal of Inorganic and Organometallic Polymers and Materials*, 2013, **23**, 787-792.
14. J. Huang, Y. Cao, Z. Liu, Z. Deng and W. Wang, *Chemical Engineering Journal*, 2012, **191**, 38-44.
15. G. H. Du, Q. Chen, R. C. Che, Z. Y. Yuan and L. M. Peng, *Applied Physics Letters*, 2001, **79**, 3702-3704.
16. S. H. Ahn, D. J. Kim, W. S. Chi and J. H. Kim, *Adv Mater*, 2013.
17. R. Rahal, A. Wankhade, D. Cha, A. Fihri, S. Ould-Chikh, U. Patil and V. Polshettiwar, *RSC Advances*, 2012, **2**, 7048.
18. S. S. Mali, C. A. Betty, P. N. Bhosale, R. S. Devan, Y.-R. Ma, S. S. Kolekar and P. S. Patil, *CrystEngComm*, 2012, **14**, 1920.
19. S. S. Mali, C. A. Betty, P. N. Bhosale and P. S. Patil, *CrystEngComm*, 2011, **13**, 6349.
20. Y. C. Chen, S. L. Lo and J. Kuo, *Water Res*, 2011, **45**, 4131-4140.
21. Y.-C. Wu and Y.-C. Tai, *Journal of Nanoparticle Research*, 2013, **15**.
22. V. Rodríguez-González, S. Obregón-Alfaro, L. M. Lozano-Sánchez and S.-W. Lee, *Journal of Molecular Catalysis A: Chemical*, 2012, **353-354**, 163-170.
23. T. Suprabha, H. G. Roy, J. Thomas, K. Praveen Kumar and S. Mathew, *Nanoscale Res Lett*, 2008, **4**, 144-152.
24. S. Yoon, E. S. Lee and A. Manthiram, *Inorganic chemistry*, 2012, **51**, 3505-3512.
25. Rajesh J. Tayade, Ramchandra G. Kulkarni and R. V. Jasra, *Industrial & Engineering Chemistry Research*, 2006, **45**, 922-927.
26. N. Sakai, Y. Ebina, K. Takada and T. Sasaki, *Journal of the American Chemical Society*, 2004, **126**, 5851-5858.
27. H. Ou and S. Lo, *Separation and Purification Technology*, 2007, **58**, 179-191.
28. X. Chen and S. S. Mao, *Chemical reviews*, 2007, **107**, 2891-2959.
29. Jacqueline bandet, Jean Frandon, Francois Fabre and B. D. Mauduit, *JAPANESE JOURNAL OF APPLIED PHYSICS*, 1993, **32**, 1518-1522.

30.   M. Gratzel, in *Solar Energy*, ed. C. L. Richter, Daniel; Gueymard, Christian A., Springer, New York, 2013, vol. XV, p. 744.